Research in Pharmaceutical Sciences, October 2023; 18(5): 517-527
Received: 08-07-2021
Peer Reviewed: 03-09-2021
Revised: 11-12-2022
Accepted: 18-01-2023
Published: 20-08-2023

School of Pharmacy & Pharmaceutical Sciences
Isfahan University of Medical Sciences

Original Article

Metabolomic identification of biochemical changes induced by fluoxetine in an insulinoma cell line (MIN6)

Surachai Ngamratanapaiboon[1,*], Krittaboon Pornchokchai[2], Siriphattarinya Wongpitoonmanachai[2], Petchlada Pholkla[2], Napatarin Srikornvit[2], Jiajun Mo[2], Patipol Hongthawonsiri[2], Pracha Yambangyang[3], and Pilaslak Akrachalanont[4]

[1]Division of Pharmacology, Department of Basic Medical Sciences, Faculty of Medicine Vajira Hospital, Navamindradhiraj University, Dusit, Bangkok, 10300, Thailand.
[2]Faculty of Medicine Vajira Hospital, Navamindradhiraj University, Dusit, Bangkok, 10300, Thailand.
[3]Department of Biomedical Engineering, Faculty of Engineering, Mahidol University, Salaya, Nakhon Pathom, 73170, Thailand.
[4]Department of Medical Sciences, Ministry of Public Health, Nonthaburi, 1100, Thailand.

Abstract

Background and purpose: The use of fluoxetine raises the risk of pancreatic beta-cell dysfunction. However, the specific mechanism behind its mechanism of action in beta cells is unknown. This study investigated the cellular response of MIN6 cells to fluoxetine using untargeted cell-based metabolomics.
Experimental approach: Metabolic profiling of MIN6 cells was performed using liquid chromatography-high resolution mass spectrometry (LC-HRMS) analysis on samples prepared under optimized conditions, followed by principal component analysis, partial least squares-discriminant analysis, and pair-wise orthogonal projections to latent structures discriminant analyses.
Findings/Results: Sixty-six metabolites that had been differentially expressed between the control and fluoxetine-treated groups demonstrated that the citric acid cycle is mainly perturbed by fluoxetine treatment.
Conclusion and implications: The current study provides insights into the molecular mechanisms of fluoxetine effects in MIN6 cells.

Keywords: Fluoxetine; High-resolution mass spectrometry; Insulinoma cell line; Liquid chromatography; Metabolomics.

INTRODUCTION

Depression is a prevalent complex psychiatric disorder characterized by low mood and a loss of pleasure (1-3). This disorder is a major cause of disability in children and adolescents and can result in difficulties in social functioning and suicide (2). To alleviate this problem, patients may be prescribed antidepressants. One of the widely prescribed antidepressants is fluoxetine; however, the use of fluoxetine raises the risk of pancreatic beta cell dysfunction (4-6) and the cellular mechanisms remain unknown.

The insulinoma cell line MIN6 model is a valuable cell model for studying the molecular mechanism of drugs in pancreatic beta cells, given that the model cells mimic several beta cell functions of humans. In this study, MIN6 cells were exposed to fluoxetine with a concentration similar to that measured in patients (7,8). Following treatment, many biochemical changes subsequently occur, which are reversible with fluoxetine treatment (5,9). Therefore, the MIN6 model of beta cell function is considered suitable for investigating the effect of fluoxetine on the molecular mechanism of pancreatic beta cells (7-9).

Access this article online	
	Website: http://rps.mui.ac.ir
	DOI: 10.4103/1735-5362.383707

*Corresponding author: S. Ngamratanapaiboon
Tel: +66-02-244-3846 ext. 5827, Fax: +66-02-244-3847
Email: surachai.n@nmu.ac.th

The concept of untargeted cell-based metabolomics allows the monitoring of metabolites in a biochemical reaction of interest (10). Normally, this method uses a liquid chromatographic separation, such as hydrophilic interaction chromatography (HILIC), before detection with mass spectrometry (MS), with minimal metabolite isolation after sampling. This technique can provide an effective, investigative, and qualitative approach to studying biological metabolism in cells, giving the best knowledge of changes to cellular metabolite concentrations (11-13).

This study aimed to investigate the cellular response of MIN6 cells to fluoxetine using HILIC-LC-MS-based untargeted metabolomics. To evaluate the cellular effects of this drug, a short-term reaction response was observed and the biological pathways involved in fluoxetine were also investigated.

MATERIALS AND METHODS

Chemicals

MS grade acetonitrile and methanol were purchased from Fisher Chemicals (Apex Chemicals, Bangkok, Thailand). Water was obtained from Elga Purelab Genetic (Rcilabscan, Bangkok, Thailand). Formic acid (MS grade) was purchased from Acros Organics (DKSH Group, Bangkok, Thailand), and all chemical compounds used were purchased from Sigma-Aldrich (Merck, Bangkok, Thailand). These chemical compounds are all MS grade.

Cell culture experiments

Cytotoxicity test

MIN6 cells (a murine pancreatic beta cell line; passages 10-13) were seeded in 96-well plates at 1×10^4 cells/well density. Cells were allowed to attach for 24 h. After reaching 70% confluency, the old medium was replaced with the new medium alone (control group), cell medium containing glucose (treated group), or cell medium containing 6 µL of 10 mM fluoxetine (treated). After 48 h, cell viability was determined using the MTS assay (Gibthai, Bangkok, Thailand) according to the manufacturer's instructions.

Cell experiment

MIN6 cells were cultured as previously described by Cataldo *et al*. (14). Briefly, MIN6 lines (passage 10-13) were treated with 20 µL of 1 M glucose for 7 min to reach a 10 mM final concentration. The concentration and time treatment give a maximal insulin secretion, in line with previous reports of glucose-stimulated insulin secretion in islets and INS-1 832/13 cells (14). The glucose-treated cells were then exposed to 6 µL of glucose solution as vehicle control or 6 µL of 10 mM fluoxetine to obtain a final concentration of 30 µM. Each group had six biological replicates. After treatment, MIN6 cells were transferred to fresh Eppendorf tubes and centrifuged for 2 min at 1,000 rpm to stop the reaction. MIN6 cell pellets were extracted with cold methanol (4 °C) and the cell suspensions vortexed for 2 h in a cold room (4 °C). The suspensions were centrifuged for 10 min at 15,000 rpm at 4 °C. The supernatants were transferred to new Eppendorf tubes and kept at -80 °C for further analysis.

Insulin assay

According to the above protocol, the insulin concentration of each condition was quantified using mouse/rat insulin ELISA kits (Merck, Bangkok, Thailand) according to the manufacturer's instructions. Summary statistics are expressed as mean ± SEM, at least three independent experiments.

Liquid chromatography-high resolution MS (LC-HRMS) analysis

Liquid chromatography was performed using the Thermo Scientific Accela LC systems coupled with the high-resolution MS Q-Exactive™ (Scispec, Bangkok, Thailand). HILIC separations were achieved using a ZIC-pHILIC column (Merck, Bangkok, Thailand) with a 150 x 2.1 mm, 3.5 µm particle size, equipped with a ZIC-pHILIC PEEK guard column (Merck, Bangkok, Thailand) with a 20 × 2.1 mm, 5 µm particle size. The mobile phases were acetonitrile (A) and 20 mM ammonium carbonate (pH 9.2) (B) at the flow rate of 0. 20 mL/minute at 40°C. At t=0 minutes run, at 5% B, a gradient to 95% B was concluded at 13 minutes and a gradient to 5% B was completed at 15 minutes. Following column wash and equilibration, the run was

concluded with 5% B at 20 minutes. Ion detection data were acquired between 70 to 1,000 m/z in ESI positive and negative modes. The pooled quality control (QC) sample was obtained by taking a 10 µL aliquot of all samples from the study and the pooled QC sample was injected during analysis and used to assess instrument performance. The details of the LC and HRMS conditions followed the same protocol as in a study by Ngamratanapaiboon et al. (10).

Data processing and statistical analysis

Manual inspection and duplicate removal were performed to form final data using Xcalibur software (Scispec, Bangkok, Thailand). LC-HRMS data were pre-processed (filtering and alignment with QC data) and extracted using Progenesis QI software (Agilent Technologies, Bangkok, Thailand). The extracted m/z data was exported to text file data for further analysis. Statistical analyses were performed using univariate (Student's T-Test) and multivariate (OPLS-DA) approaches. Simca P software (Sartorius, Goettingen, Germany) was also used for statistical analyses. Detected ions were pre-selected as candidates when their variable importance for projection (VIP) values were > 1.00. The VIP value indicates the importance of each metabolite for group separation. The detected ions with a p-value < 0.05 (T-test) were identified as significantly changed ions with the strongest correlation with the OPLS-DA discriminant scores to decrease the risk of false positives when selecting potentially significantly detected ions. The p-value describes a measure of the likelihood that the association between a set of metabolites in the dataset and a related function is random. In general, a p-value < 0.05 indicates a statistically significant, non-random association. In addition, features that were detected in every chromatogram and had < 30% of covariants with each group were included in the analysis.

Metabolite identification

The identification of significantly altered ions was confirmed with authentic standards that are available in our laboratory using standard peak assignment or SRM. Some metabolites were tentatively identified through an accurate mass search of the Human Metabolome database (https://hmdb.ca/) and the METLIN database (https://metlin.scripps.edu) with a mass error of less than 5 ppm.

Metabolic pathway analysis

The results of the probable pathway analysis with MetaboAnalyst 5.0 software (https://www.metaboanalyst.ca/) and the previous publication results were integrated to help identify the most relevant pathways implicated in the conditions under investigation.

RESULTS

Cell viability and insulin secretion

In the MTS assay, it was found that the MIN6 cell viability was not affected by 10 mM glucose or 30 µM fluoxetine compared to the control as shown in Fig. 1A. The effect of glucose and the combination of glucose and fluoxetine on insulin secretion were analyzed. As shown in Fig. 1B, the insulin concentration increased with the glucose and the combination of glucose and fluoxetine compared with the control. However, the insulin concentration was reduced by fluoxetine in MIN6 cells compared to the group that received glucose only.

LC-HRMS analysis

To check instrument performance, 5 µL of each sample was pooled to generate a QC sample. MS spectral data (Figs. S1 and S2) were aligned using the QC samples. Importantly, the alignment process was applied to the aligned data to identify significant clusters in an unsupervised manner and did not affect the clustering of the samples. Furthermore, to minimize any metabolic changes caused by environmental factors, the pooled samples (QC) were used for normalizing the data. Based on mass alignment with a mass spectral database and comparison with authentic standards and data from the literature, 173 metabolites were identified in this study, including amino acids, fatty acids, organic acids, and sugars (data not shown). Figure 2 shows the extracted MS peak chromatogram of some detected metabolites.

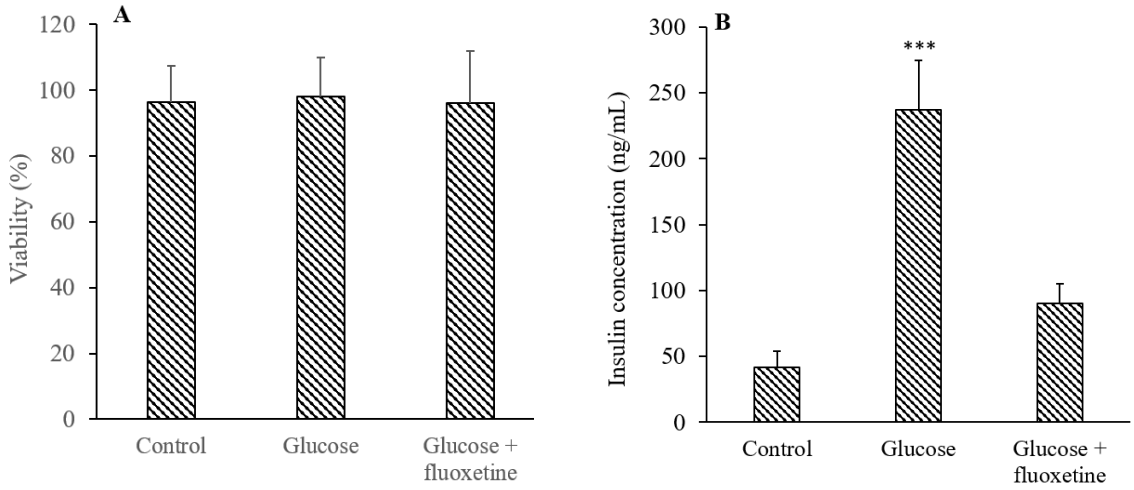

Fig. 1. (A) The percentage viability and (B) the insulin concentration of the MIN6 cells treated with cell medium alone (control), the glucose (10 mM), or the combination of glucose (10 mM) and fluoxetine (30 µM). Data are expressed as percentage of control cells and each bar is represented as mean ± SD of triplicates (n = 3) ***P < 0.001 Indicates significant difference in comparison with the control group.

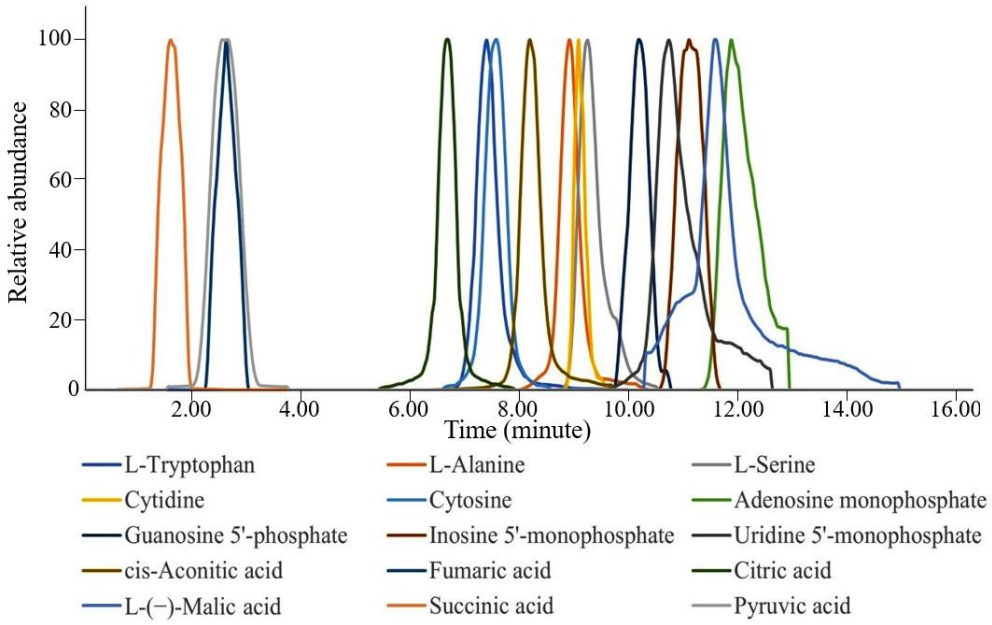

Fig. 2. Extracted mass spectrometry peak chromatogram of some detected metabolites.

Multivariate statistical analysis of the metabolomics data

A principal component analysis (PCA) was used to visualize general clustering, trend, or outliers among the studies. Score plot and model analysis including Hoteling's T2 plot showed no outliers. As seen in Fig. 3A, QC groups were clustered, which suggests that the quality of data was acceptable. In the PCA score plot, fluoxetine treatment samples were separated from the control groups.

OPLS-DA was applied to better understand the different metabolic patterns and to detect potentially significant metabolites showing prominent concentration changes in the models. The quality of the results of discriminant models was R^2 = 0.99965 and Q^2 = 0.99292. The key model parameters, R^2 and Q^2 between control and fluoxetine treatment, were larger than 0.5, suggesting that this study was robust and had good fitness and prediction. The control groups were clearly distinguished in the OPLS-DA plot (Fig. 3B). The figure showed that fluoxetine-treated groups had distinctive metabolic profiles from the control and glucose groups.

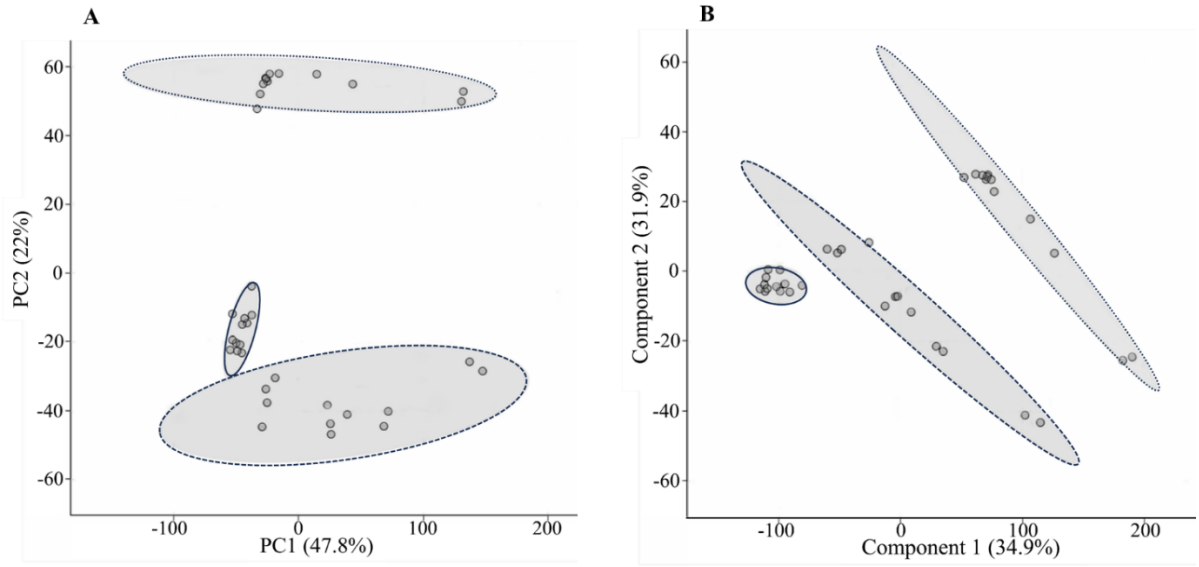

Fig. 3. (A) PCA scores plot and (B) orthogonal partial squares discriminant analysis scores plot of the cell medium alone (round dot oval), glucose (square dot oval), and combination of glucose and fluoxetine groups (solid oval). PCA, Principal component analysis.

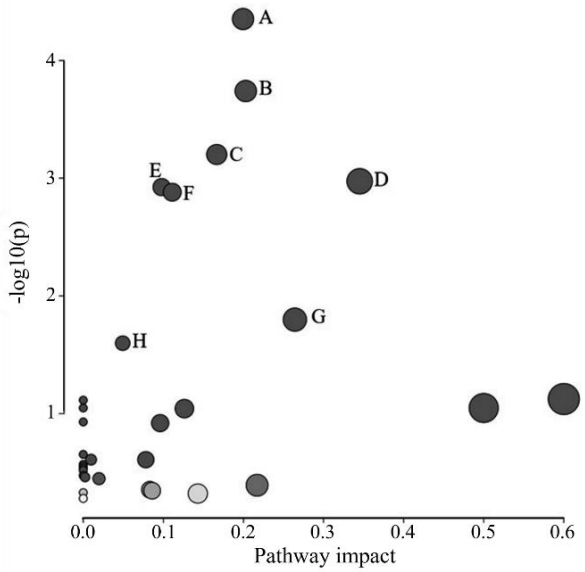

Fig. 4. Pathway analysis overview depicting altered metabolic pathways in MIN6 cells from control and 10 mM glucose + 30 μM fluoxetine-treated groups. The metabolic pathways are displayed as distinct circles depending on their enrichment analyses scores (vertical axis and topology (pathway impact, horizontal axis, circle diameter) *via* MetaboAnalyst 5.0. A: Alanine, aspartate, and glutamate metabolism; B: citrate cycle (TCA cycle); C: aminoacyl-tRNA biosynthesis; D: arginine biosynthesis; E: glyoxylate and dicarboxylate metabolism; F: butanoate metabolism; G: purine metabolism; and H: tyrosine metabolism.

Significantly altered metabolites for fluoxetine effects

The OPLS-DA VIP with Student's T-Test was used for selecting significant metabolites responsible for group separation. Metabolites were pre-selected as candidates when their VIP values were larger than 1.0. Then, among these, metabolites where $P < 0.05$ (Table S1) were selected as metabolites that were most correlated with the OPLS-DA discriminant scores in order to decrease the risk of false positives in the selection of most significantly altered metabolites. Sixty-six metabolites were selected as potentially altered metabolite markers in MIN6 cells exposed to fluoxetine compared with the control group (10 mM glucose treatment).

Analysis of metabolic pathways

Metaboanalyst 5.0 (https://www.metaboanalyst.ca/MetaboAnalyst/home.xhtml) and the selected metabolites were used to analyze metabolic pathways. Compared with the control group, 31 metabolic pathways were affected (data not shown) in the 30 μM fluoxetine-treated group. Of these, a markedly perturbated pathway was filtered according to specific criteria ($P < 0.05$ and impact value greater than 0.2): TCA cycle ($P = 0.000$ and impact = 0.264). The metabolic pathway was represented by a colored circle within the diagram (Fig. 4).

DISCUSSION

Fluoxetine is reported to be associated with both hyperglycemia and an increased risk of

type 2 diabetes (15,16). The glucose-stimulated insulin secretion of beta cells is mainly controlled by glycolysis and the TCA cycle pathways (17). Untargeted metabolomics using the LC-HRMS approach was applied to MIN6 cells to gain insight into the molecular mechanisms of the effect of fluoxetine.

Untargeted cell-based metabolomics using LC-HRMS were used to further uncover the likely mechanisms underlying the effect of fluoxetine in MIN6 cells. This approach led to the identification of 66 differential metabolites in the 30 μM fluoxetine-treated group compared with the control (Table S1). Among these metabolites, 25 were selected as the most significantly altered. The TCA cycle was the most significantly disturbed by exposure to fluoxetine. A schematic diagram of the modulated metabolites and potential disturbed metabolic pathways is shown in Fig. 5.

Glucose-induced insulin secretion is controlled by a signal generated in the mitochondria (18). The vital key signal is ATP, which is produced from bioenergetics processes (glycolysis, TCA cycle and electron transport chain (ETC)) in the mitochondria. The elevation of ATP concentration is important for the trigger of insulin exocytosis (19). Bioenergetic compounds, such as pyruvic acid, (iso)citric acid, and fumaric acid, Table S1, were identified in the fluoxetine-treated group compared with the control group. Specifically, increases in fumaric acid, succinic acid, malate, cis-aconitic acid, and citric acid, which are associated with the TCA cycle, were observed. Activation of the TCA cycle results in the production of vital electrons that are transferred to the ETC, resulting in the generation of ATP (19,20). Kao *et al*. found that fluoxetine increases TCA cycle activity in mice through mitochondrial function (21).

De Long *et al.* have suggested that fluoxetine may contribute to decreased mitochondrial ETC enzyme activity and reduced glucose-stimulated insulin secretion. In combination with the current results, it may be that fluoxetine may reduce glucose-stimulated insulin secretion by affecting ATP generation through the inhibition of the ETC in mitochondria. This inhibition results in increased levels of TCA intermediate metabolites (5).

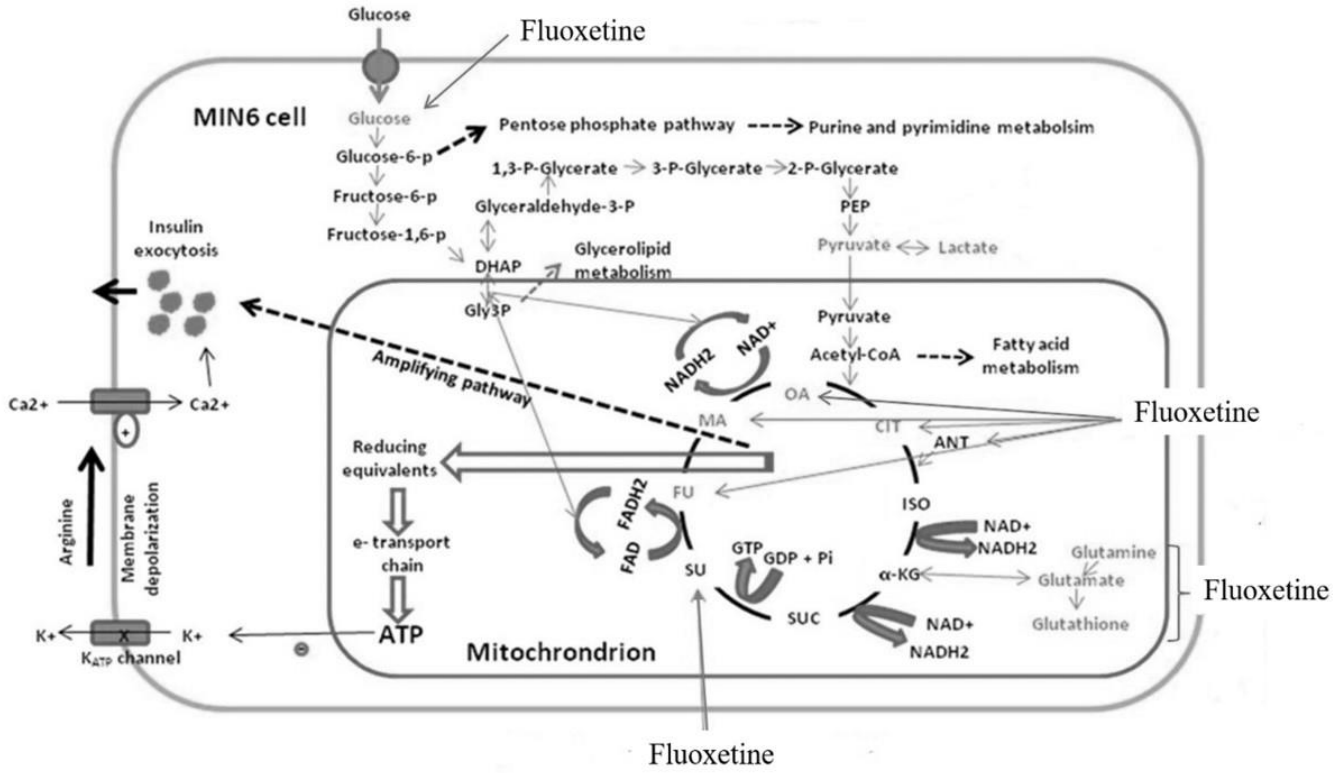

Fig. 5. Model for the coupling of glucose metabolism to insulin secretion and the effects of fluoxetine on MIN6 cells.

While the observation of MIN6 cells through the use of untargeted metabolomics and LC-HRMS approach may not be fully applicable to islets, this study has several advantages over *in vivo* studies and more precise measurements due to the ease of manipulation and procurement. One limitation of these studies is the lack of accurate measurement to identify all the glycolysis, TCA, and ETC intermediate metabolites not detected by the method used, and incomplete authentic standards that may be used for confirmation. To address this limitation, a targeted metabolic profile could be used to cover only interested metabolites and MS/MS fragmentation should be used to identify and confirm detected metabolites.

CONCLUSION

Data generated using an untargeted metabolomics-based LC-HRMS approach to study the fluoxetine effects in MIN6 cells has demonstrated a method to test and extend several hypotheses for studying the effects of drugs and other compounds on the biochemical mechanisms of beta cell function. The measurement of intermediate metabolites of glycolysis, the TCA cycle, ETC, amino acids, lipids, and other compounds, known as a metabolic profile, shows an interaction of metabolites that are vital in both triggering and amplifying pathways of beta cell function, thus helping to refine the global view. Support for the energy metabolism hypothesis comes from measurements in the study that confirm previous findings and reveal the exact biological pathways. Finally, it was clear that fluoxetine affects the TCA cycle in the mitochondria of MIN6 cells.

Acknowledgements

We would like to thank Paul A. Smith (School of Life Science, University of Nottingham Medical School, Queens Medical Centre, Nottinghamshire, NG7 2UH, UK) for providing us with MIN6 cells. The authors are also grateful to the Research Facilitation Division, Faculty of Medicine Vajira Hospital, Navamindradhiraj University, for the proofreading fee.

Conflict of interest statement

The authors declared no conflict of interest in this study.

Authors' contribution

S. Ngamratanapaiboon conceptualized, designed, and performed experimental parts of the study, analyzed the data, and wrote the manuscript; K. Pornchokchai, S. Wongpitoonmanachai, P. Pholkla, N. Srikornvit, J. Mo, and P. Hongthawonsiri performed cell viability and insulin measurement, and analyzed the data; P. Yambangyang and P. Akrachalanont performed experimental parts of the study. The finalized article was approved by all authors.

REFERENCES

1. Carratalá-Ros C, López-Cruz L, Martínez-Verdú A, Olivares-García R, Salamone JD, Correa M. Impact of fluoxetine on behavioral invigoration of appetitive and aversively motivated responses: interaction with dopamine depletion. Front Behav Neurosci. 2021;15:700182,1-15.
   DOI: 10.3389/fnbeh.2021.700182.
2. Reyad AA, Plaha K, Girgis E, Mishriky R. Fluoxetine in the management of major depressive disorder in children and adolescents: a meta-analysis of randomized controlled trials. Hosp Pharm. 2020;56(5):525-531.
   DOI: 10.1177/0018578720925384.
3. Zhao J, Jung YH, Jang CG, Chun KH, Kwon SW, Lee J. Metabolomic identification of biochemical changes induced by fluoxetine and imipramine in a chronic mild stress mouse model of depression. Sci Rep. 2015;5:8890,1-8.
   DOI: 10.1038/srep08890.
4. Chang HY, Chen SL, Shen MR, Kung ML, Chuang LM, Chen YW. Selective serotonin reuptake inhibitor, fluoxetine, impairs E-cadherin-mediated cell adhesion and alters calcium homeostasis in pancreatic beta cells. Sci Rep. 2017;7:3515,1-13.
   DOI: 10.1038/s41598-017-03747-0.
5. De Long NE, Hyslop JR, Raha S, Hardy DB, Holloway AC. Fluoxetine-induced pancreatic beta cell dysfunction: new insight into the benefits of folic acid in the treatment of depression. J Affect Disord. 2014;166:6-13.
   DOI: 10.1016/j.jad.2014.04.063.
6. Elmorsy E, Alelwani W, Kattan S, Babteen N, Alnajeebi A, Ghulam J, *et al*. Antipsychotics inhibit the mitochondrial bioenergetics of pancreatic beta cells isolated from CD1 mice. Basic Clin Pharmacol Toxicol. 2021;128(1):154-168.
   DOI: 10.1111/bcpt.13484.

7. Sagahón-Azúa J, Medellín-Garibay SE, Chávez-Castillo CE, González-Salinas CG, Milán-Segovia RDC, Romano-Moreno S. Factors associated with fluoxetine and norfluoxetine plasma concentrations and clinical response in Mexican patients with mental disorders. Pharmacol Res Perspect. 2021;9(5):e00864,1-10.
   DOI: 10.1002/prp2.864.
8. Keyvanloo Shahrestanaki M, Aghaei M. A3 receptor agonist, Cl-IBMECA, potentiate glucose-induced insulin secretion from MIN6 insulinoma cells possibly through transient Ca^{2+} entry. Res Pharm Sci. 2019;14(2):107-114.
   DOI: 10.4103/1735-5362.253357.
9. Elmorsy E, Al-Ghafari A, Almutairi FM, Aggour AM, Carter WG. Antidepressants are cytotoxic to rat primary blood brain barrier endothelial cells at high therapeutic concentrations. Toxicol In Vitro. 2017;44:154-163.
   DOI: 10.1016/j.tiv.2017.07.011.
10. Ngamratanapaiboon S, Yambangyang P. Quantification of antipsychotic biotransformation in brain microvascular endothelial cells by using untargeted metabolomics. Drug Discov Ther. 2021;15(6):317-324.
    DOI: 10.5582/ddt.2021.01101.
11. Ahangarpour A, Shabani R, Farbood Y. The effect of betulinic acid on leptin, adiponectin, hepatic enzyme levels and lipid profiles in streptozotocin-nicotinamide-induced diabetic mice. Res Pharm Sci. 2018;13(2):142-148.
    DOI: 10.4103/1735-5362.223796.
12. Collette TW, Ekman DR, Zhen H, Nguyen H, Bradley PM, Teng Q. Cell-based metabolomics for untargeted screening and prioritization of vertebrate-active stressors in streams across the United States. Environ Sci Technol. 2019;53(15):9232-9240.
    DOI: 10.1021/acs.est.9b02736.
13. Wright Muelas M, Roberts I, Mughal F, O'Hagan S, Day PJ, Kell DB. An untargeted metabolomics strategy to measure differences in metabolite uptake and excretion by mammalian cell lines. Metabolomics. 2020;16(10):107,1-12.
    DOI: 10.1007/s11306-020-01725-8.
14. Cataldo LR, Cortés VA, Mizgier ML, Aranda E, Mezzano D, Olmos P, *et al*. Fluoxetine impairs insulin secretion without modifying extracellular serotonin levels in MIN6 *β*-cells. Exp Clin Endocrinol Diabetes. 2015;123(8):473–478.
    DOI: 10.1055/s-0035-1549964.
15. Roopan S, Larsen ER. Use of antidepressants in patients with depression and comorbid diabetes mellitus: a systematic review. Acta Neuropsychiatr. 2017;29(3):127-139.
    DOI: 10.1017/neu.2016.54.
16. Biagetti B, Corcoy R. Hypoglycemia associated with fluoxetine treatment in a patient with type 1 diabetes. World J Clin Cases. 2013;1(5):169-171.
    DOI: 10.12998/wjcc.v1.i5.169.
17. Jensen MV, Joseph JW, Ronnebaum SM, Burgess SC, Sherry AD, Newgard CB. Metabolic cycling in control of glucose-stimulated insulin secretion. Am J Physiol Endocrinol Metab. 2008;295(6):E1287-E1297.
    DOI: 10.1152/ajpendo.90604.2008.
18. Maechler P, Wollheim CB. Mitochondrial signals in glucose-stimulated insulin secretion in the beta cell. J Physiol. 2000;529(Pt1):49-56.
    DOI: 10.1111/j.1469-7793.2000.00049.x.
19. Tengholm A. Cyclic AMP dynamics in the pancreatic *β*-cell. Ups J Med Sci. 2012;117(4):355-369.
    DOI: 10.3109/03009734.2012.724732.
20. Bonora M, Patergnani S, Rimessi A, De Marchi E, Suski JM, Bononi A, *et al*. ATP synthesis and storage. Purinergic Signal. 2012;8(3):343-357.
    DOI: 10.1007/s11302-012-9305-8.
21. Kao CY, He Z, Henes K, Asara JM, Webhofer C, Filiou MD, *et al*. Fluoxetine treatment rescues energy metabolism pathway alterations in a posttraumatic stress disorder mouse model. Mol Neuropsychiatry. 2016;2(1):46-59.
    DOI: 10.1159/000445377.

Supplementary illustrations

Table S1. Significantly changed metabolites in MIN6 cells treated with fluoxetine.

Putative metabolites	Formula	Monoisotopic molecular weight	Retention time (min)	Confirmation	VIP	*P*-Value	Fold change (fluoxetine/control)
Ganglioside GA2 (d18:1/24:0)	$C_{62}H_{116}N_2O_{18}$	1176.8223	2.13	Mass error < 3 ppm	1.05	0.00	0.00
Lysophosphoethanolamine	$C_{25}H_{50}NO_7P$	507.3325	2.10	Mass error < 3 ppm	1.05	0.00	0.00
Lysophosphocholine	$C_{34}H_{68}NO_7P$	633.4733	2.13	Mass error < 3 ppm	1.02	0.00	0.00
Dodecanedioic acid	$C_{12}H_{22}O_4$	230.1518	2.21	Mass error < 3 ppm	1.03	0.00	0.01
Ceramide phosphate	$C_{32}H_{64}NO_6P$	589.4471	2.13	Mass error < 3 ppm	1.04	0.00	0.01
Cardiolipin	$C_{85}H_{148}O_{17}P_2$	1503.0192	2.19	Mass error < 3 ppm	1.02	0.00	0.01
Glucosylsphingosine	$C_{24}H_{47}NO_7$	461.3353	2.13	Mass error < 3 ppm	1.04	0.00	0.02
Thyroxine glucuronide	$C_{21}H_{19}I_4NO_{10}$	952.7188	2.13	Mass error < 3 ppm	1.04	0.00	0.02
Lysophosphoethanolamine	$C_{27}H_{56}NO_7P$	537.3794	2.19	Mass error < 3 ppm	1.04	0.00	0.05
Ganglioside GD1B	$C_{85}H_{149}N_3O_{39}$	1835.9768	2.19	Mass error < 3 ppm	1.03	0.00	0.06
Adenosine monophosphate	$C_{10}H_{14}N_5O_7P$	347.0631	8.22	Authentic standard	1.06	0.00	0.27
Inosine 2',3'-cyclic phosphate	$C_{10}H_{11}N_4O_7P$	330.0365	8.04	Authentic standard	1.05	0.00	0.29
Guanosine monophosphate	$C_{10}H_{14}N_5O_8P$	363.0580	9.42	Authentic standard	1.06	0.00	0.50
N-Acetyl-D-glucosamine 6-phosphate	$C_8H_{16}NO_9P$	301.0563	8.70	Mass error < 3 ppm	1.11	0.00	0.56
9'-Carboxygamma-tocotrienol	$C_{23}H_{32}O_4$	372.2301	2.30	Mass error < 3 ppm	1.10	0.00	0.69
Myristic acid	$C_{14}H_{28}O_2$	228.2089	2.60	Authentic standard	1.06	0.00	0.76
8E-Heptadecenedioic acid	$C_{17}H_{30}O_4$	298.2144	1.86	Mass error < 3 ppm	1.03	0.00	0.84
Cytosine	$C_4H_5N_3O$	111.0433	7.61	Authentic standard	1.05	0.00	0.93
Cytidine	$C_9H_{13}N_3O_5$	243.0855	7.61	Authentic standard	1.01	0.00	0.94
Nicotinamide ribotide	$C_{11}H_{16}N_2O_8P$	335.0644	7.37	Mass error < 3 ppm	1.01	0.00	1.04
2,3-dinor-PGE1	$C_{18}H_{30}O_5$	326.2093	1.95	Mass error < 3 ppm	1.05	0.00	1.06
Galactinol	$C_{12}H_{22}O_{11}$	342.1162	9.33	Mass error < 3 ppm	1.03	0.00	1.09
N1, N12-Diacetylspermine	$C_{14}H_{30}N_4O_2$	286.2369	2.30	Mass error < 3 ppm	1.05	0.00	1.12
CerP(d18:1/26:1(17Z))	$C_{46}H_{90}NO_6P$	783.6506	2.60	Mass error < 3 ppm	1.04	0.00	1.13
2-Hexenoylcholine	$C_{11}H_{22}NO_2$	200.1651	2.47	Mass error < 3 ppm	1.03	0.00	1.18
Triglyceride	$C_{52}H_{100}O_5$	804.7571	14.67	Mass error < 3 ppm	1.04	0.00	1.21
L-Tryptophan	$C_{11}H_{12}N_2O_2$	204.0899	7.75	Authentic standard	1.03	0.00	1.30
Guanosine	$C_{10}H_{13}N_5O_5$	283.0917	8.04	Authentic standard	1.01	0.00	1.64
L-Methionine	$C_5H_{11}NO_2S$	149.0510	7.63	Authentic standard	1.09	0.00	1.71
Tyramine	$C_8H_{11}NO$	137.0841	7.22	Authentic standard	1.10	0.00	1.77
Uridine diphosphate-N-acetylglucosamine	$C_{17}H_{27}N_3O_{17}P_2$	607.0816	8.67	Mass error < 3 ppm	1.02	0.00	1.77
2'-Inosine-5'-monophosphate	$C_{10}H_{13}N_4O_8P$	348.0471	8.87	Authentic standard	1.09	0.00	1.95
Uridine diphosphate glucuronic acid	$C_{15}H_{22}N_2O_{18}P_2$	580.0343	10.23	Mass error < 3 ppm	1.06	0.00	2.09
Phosphocholine	$C_{56}H_{102}N_2O_{18}$	955.7969	1.74	Mass error < 3 ppm	1.02	0.00	2.23
L-Gluconolactone	$C_6H_{10}O_6$	178.0477	2.12	Authentic standard	1.10	0.00	2.35

Table S1. (Continued)

Putative metabolites	Formula	Monoisotopic molecular weight	Retention time (min)	Confirmation	VIP	*P*-Value	Fold change (fluoxetine/control)
L-Glutamic acid	$C_5H_9NO_4$	147.0532	8.47	Authentic standard	1.01	0.00	2.40
L-Alanine	$C_3H_7NO_2$	89.0477	8.87	Authentic standard	1.04	0.00	2.48
Triglyceride	$C_{68}H_{114}O_6$	1026.8615	2.60	Mass error < 3 ppm	1.05	0.00	2.60
Triglyceride	$C_{62}H_{106}O_5$	930.8040	2.16	Mass error < 3 ppm	1.06	0.00	2.64
Uridine 5'-monophosphate	$C_9H_{13}N_2O_9P$	324.0359	8.67	Authentic standard	1.09	0.00	2.76
L-Serine	$C_3H_7NO_3$	105.0426	9.33	Authentic standard	1.04	0.00	2.78
N4-Acetylaminobutanal	$C_6H_{11}NO_2$	129.0790	7.94	Mass error < 3 ppm	1.04	0.00	2.80
3-Hydroxytetradecanedioic acid	$C_{14}H_{26}O_5$	274.1780	2.27	Mass error < 3 ppm	1.02	0.00	2.89
Succinyladenosine	$C_{14}H_{17}N_5O_8$	383.1077	8.45	Mass error < 3 ppm	1.03	0.00	3.06
Succinic acid	$C_4H_6O_4$	118.0266	8.24	Authentic standard	1.05	0.00	3.51
Pivaloylcarnitine	$C_{12}H_{23}NO_4$	245.1627	6.48	Mass error < 3 ppm	1.02	0.00	4.69
2-Hydroxyundecanoic acid	$C_{11}H_{22}O_3$	202.1569	2.30	Mass error < 3 ppm	1.07	0.00	4.71
N-Stearoyl histidine	$C_{24}H_{43}N_3O_3$	421.3304	1.74	Mass error < 3 ppm	1.13	0.00	5.23
Citric acid	$C_6H_8O_7$	192.0270	9.84	Authentic standard	1.02	0.00	5.53
Triglyceride	$C_{73}H_{134}O_6$	1107.0180	2.21	Mass error < 3 ppm	1.03	0.00	5.55
Citrulline	$C_6H_{13}N_3O_3$	175.0957	9.45	Authentic standard	1.12	0.00	5.59
3-Oxotetradecanoic acid	$C_{14}H_{26}O_3$	242.1882	2.44	Mass error < 3 ppm	1.09	0.00	5.69
Isobutyryl carnitine	$C_{11}H_{22}NO_4$	232.1543	6.65	Mass error < 3 ppm	1.06	0.00	6.08
Uridine diphosphate glucose	$C_{15}H_{24}N_2O_{17}P_2$	566.0550	9.19	Authentic standard	1.09	0.00	6.21
Nicotinamide N-oxide	$C_6H_6N_2O_2$	138.0429	2.60	Mass error < 3 ppm	1.11	0.00	6.62
LysoPI(18:1(9Z)/0:0)	$C_{27}H_{51}O_{12}P$	598.3118	2.26	Mass error < 3 ppm	1.14	0.00	8.63
Diacylglycerols	$C_{31}H_{52}O_6$	520.3764	3.61	Mass error < 3 ppm	1.13	0.00	8.84
Fumaric acid	$C_4H_4O_4$	116.0110	8.87	Authentic standard	1.06	0.00	9.03
Octenoyl-L-carnitine	$C_{15}H_{27}NO_4$	285.1940	2.60	Mass error < 3 ppm	1.02	0.00	9.41
Acetoacetic acid	$C_4H_6O_3$	102.0317	8.60	Authentic standard	1.09	0.00	19.86
Malic acid	$C_4H_6O_5$	134.0215	8.82	Authentic standard	1.06	0.00	23.86
D-Glucose	$C_6H_{12}O_6$	180.0634	8.62	Authentic standard	1.10	0.00	28.84
cis-Aconitic acid	$C_6H_6O_6$	174.0164	9.27	Authentic standard	1.02	0.00	33.27
Pyroglutaric acid	$C_5H_6O_3$	114.0317	8.65	Authentic standard	1.09	0.00	38.56
3-Methylglutaconic acid	$C_6H_8O_4$	144.0423	8.65	Mass error < 3 ppm	1.09	0.00	44.46
Pregnanediol 3-O-glucuronide	$C_{27}H_{44}O_8$	496.3036	1.44	Mass error < 3 ppm	1.13	0.00	84.33

VIP, Variable importance for projection

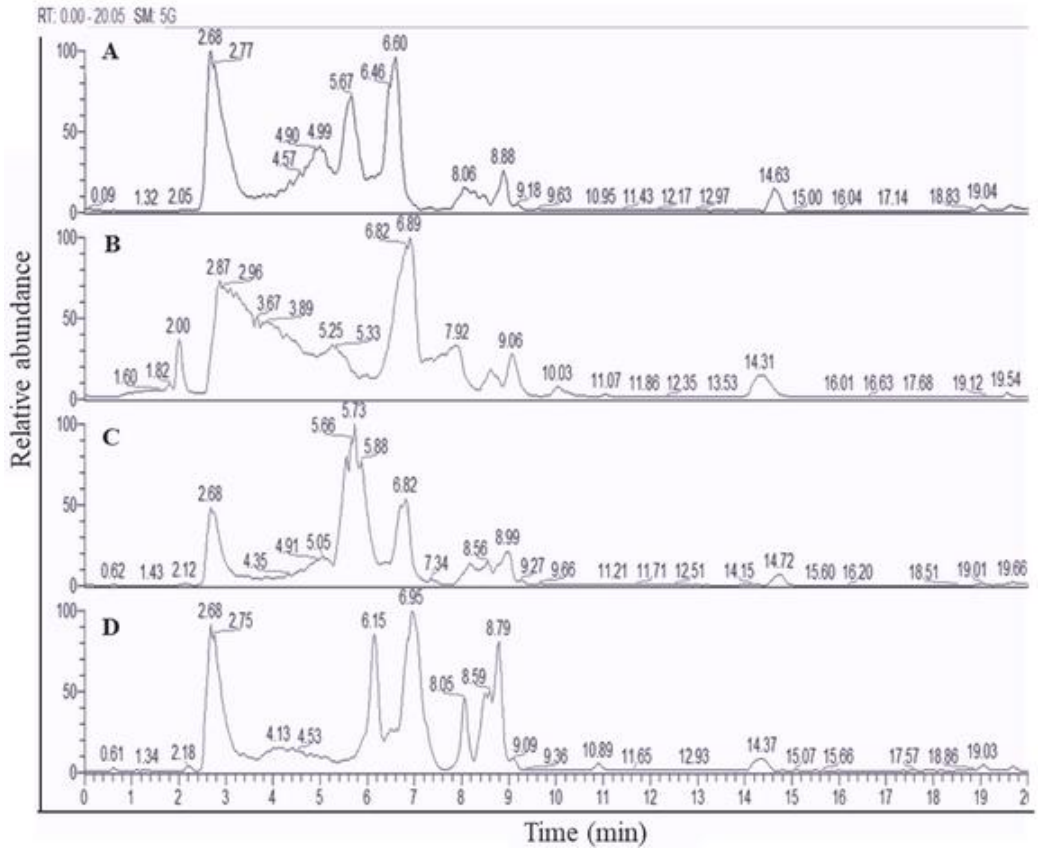

Fig. S1. Mass spectrometry base chromatograms of (A) control, (B) glucose-treated, (C) glucose + fluoxetine-treated and (D) quality control groups in positive electro-ionization mode.

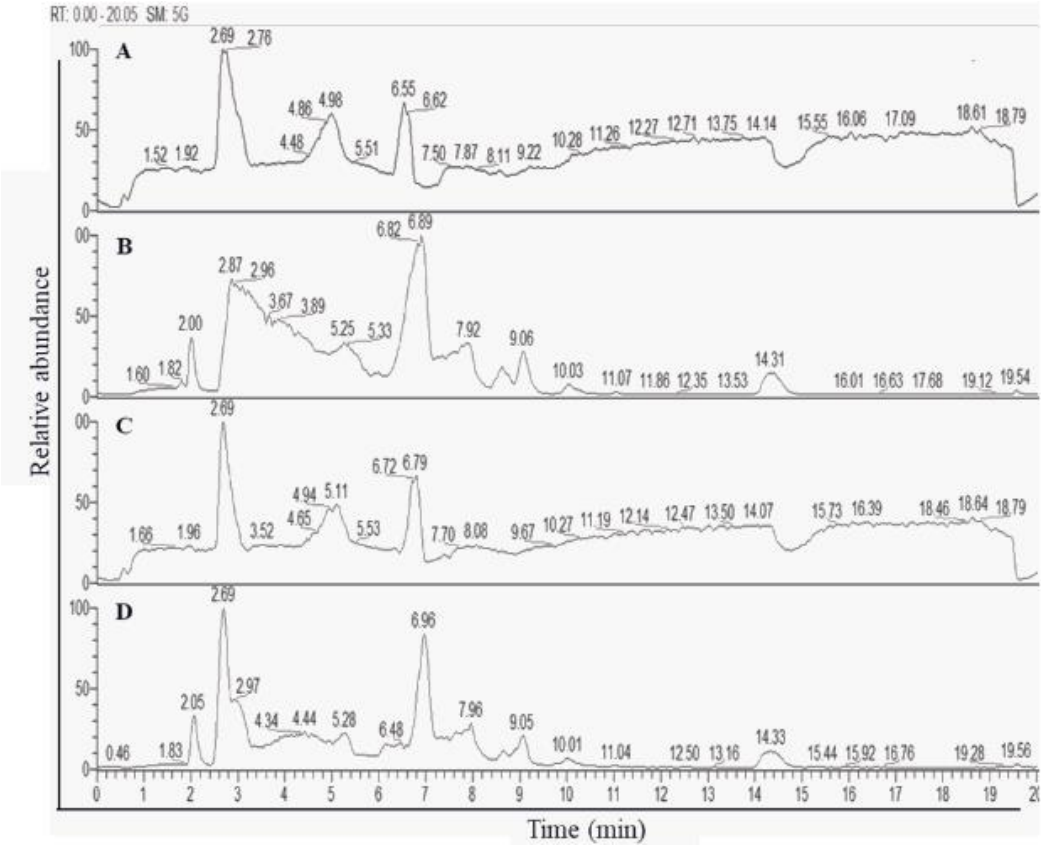

Fig. S2. Mass spectrometry base chromatograms of (A) control, (B) glucose-treated, (C) glucose + fluoxetine-treated and (D) quality control groups in negative electro-ionization mode.